Journal of CO2 Utilization 111 (2026) 103555

Contents lists available at ScienceDirect

Journal of CO2 Utilization

journal homepage: www.elsevier.com/locate/jcou

CO_2 to chemicals: evaluating the potential of Fischer-Tropsch naphthas as a circular source of light olefins

Anas Jamil Abdulrahman [a,1], Niko Heikkinen [b,1], Miia Nevander [b], Miloš Auersvald [a,c], Sphurti Prakash Kulkarni [a], Oleksii Mynko [a], Behzad Parvizi [a], Daniël Withoeck [a], Marco Huotari [b], Juha Lehtonen [b], Christian Frilund [b], Matti Reinikainen [b], Eveliina Mäkelä [b], Marvin Kusenberg [a], Kevin M. Van Geem [a,*]

[a] Laboratory for Chemical Technology (LCT), Department of Materials, Textiles and Chemical Engineering, Faculty of Engineering & Architecture, Ghent University, Zwijnaarde, B-9052, Belgium
[b] VTT Technical Research Centre of Finland, P.O. Box 1000, Espoo, 02044 VTT, Finland
[c] Department of Sustainable Fuels and Green Chemistry, University of Chemistry and Technology Prague, Prague 6, 166 28, Czech Republic

ARTICLE INFO

Keywords:
Carbon capture and utilization
Reverse Water-Gas Shift
Fischer-Tropsch synthesis
CO_2-derived feedstocks
Steam cracking
Ethylene carbon intensity

ABSTRACT

Rising industrial CO_2 emissions and the limited capacity of current abatement technologies highlight the need for scalable carbon utilization pathways. Fischer-Tropsch synthesis provides a route to convert captured CO_2 into hydrocarbon feedstocks compatible with existing petrochemical processes, such as steam cracking. However, their suitability as steam cracker feedstocks has not yet been fully demonstrated. Three Fischer-Tropsch (FT)-derived feedstocks were generated from captured CO_2 via Reverse Water-Gas Shift followed by Fischer-Tropsch synthesis. The crude FT oil (i) was hydrotreated to produce hydrotreated FT oil (ii), and subsequent distillation yielded a hydrotreated FT naphtha (iii). The feedstocks were characterized using comprehensive two-dimensional gas chromatography, benchmarked against fossil naphtha in a bench-scale steam cracker, and evaluated for their impact on the carbon intensity of ethylene production. FT-derived feedstocks were highly paraffinic and contained negligible sulfur, nitrogen, halogens, and metals. Crude FT oil contained 11.7 wt% oxygenates and 11.3 wt% olefins, which were removed by hydrotreatment, yielding more stable steam cracker feedstocks. When steam-cracking the respective oils at 880 °C, the crude FT oil produced 38% more ethylene than fossil naphtha, while the yield of pyrolysis fuel oil (C_{10+}) was halved. Further upgrading to hydrotreated FT naphtha increased the ethylene advantage to 48% and reduced pyrolysis fuel oil formation to one-third of that with fossil naphtha. The higher ethylene selectivity led to a 27% reduction in cracker-level CO_2 intensity compared with fossil naphtha. These results demonstrate that CO_2-derived FT feedstocks can serve as clean, high-yield alternatives for light olefin production within existing petrochemical infrastructure.

1. Introduction

Industrial activities over the past two centuries have significantly increased greenhouse gas emissions, with CO_2 as a dominant contributor to anthropogenic climate change [1]. Energy-intensive industries, including iron and steel, cement, and chemicals, account for the largest share of industrial CO_2 emissions and are categorized as hard-to-abate due to their high energy demands, intrinsic process emissions, and their reliance on fossil-based carbon feedstocks [2–4]. In the chemicals and petrochemicals sector, fossil feedstocks serve not only as energy sources but also as carbon building blocks in products, complicating decarbonization pathways.

Steam cracking is the dominant industrial route for producing light olefins, particularly ethylene and propylene, which are foundational to plastics, solvents, and numerous bulk chemicals. The process operates under severe thermal conditions and is highly energy-intensive, with a substantial fraction of its direct emissions arising from furnace fuel combustion, which accounts for more than 80% of Scope 1 emissions in conventional ethylene plants [5]. Electrification of steam cracking furnaces has emerged as a promising mitigation strategy [2–6]. However,

* Corresponding author.
E-mail address: Kevin.VanGeem@UGent.be (K.M. Van Geem).
[1] These authors contributed equally to this work and share first authorship.

https://doi.org/10.1016/j.jcou.2026.103555
Received 14 June 2026; Received in revised form 18 August 2026; Accepted 22 August 2026
Available online 25 August 2026
2212-9820/© 2026 The Authors. Published by Elsevier Ltd. This is an open access article under the CC BY-NC-ND license (http://creativecommons.org/licenses/by-nc-nd/4.0/).

electrification alone does not address the fossil origin of the carbon embedded in the feedstock. Consequently, replacing fossil-derived carbon with circular or renewable carbon sources is essential for achieving deep decarbonization of olefin production. In this context, feedstock composition strongly affects light olefin selectivity, secondary reaction pathways, and specific energy consumption per ton of product.

Net-zero transition scenarios project that a significant fraction of future chemical feedstocks must originate from circular and renewable carbon streams, including captured CO_2 [7,8]. Carbon capture and utilization technologies aim to convert CO_2 emissions into valuable chemical intermediates. Nevertheless, global deployment remains limited, with only a small fraction of emitted CO_2 currently being captured and utilized [9]. Scalable valorization routes that integrate with existing petrochemical infrastructure are therefore required to enable meaningful CO_2 utilization in the chemical sector. Among the thermochemical conversion pathways that can integrate with existing petrochemical infrastructure, Fischer-Tropsch synthesis is a particularly promising option. It is an industrially established catalytic process that converts synthesis gas into a broad spectrum of hydrocarbons. Historically, it has been deployed in regions where conventional crude oil resources were limited, but alternative carbonaceous feedstocks were available. This flexibility has enabled large-scale commercialization worldwide, including coal-based facilities in South Africa operated by Sasol [10,11], natural gas-based plants in Qatar operated by ExxonMobil [12], and facilities in Malaysia operated by Shell [13]. Beyond conventional fossil-derived syngas routes, FT synthesis has gained renewed attention as a platform for sustainable fuel and chemical production due to its compatibility with non-fossil carbon sources. Biomass, residual wastes, and CO_2 can be converted into synthesis gas and subsequently upgraded via FT synthesis to produce synthetic hydrocarbons [14–16]. The FT process inherently produces a distribution of products whose composition depends on catalyst type and operating conditions, typically yielding a synthetic crude that requires downstream upgrading and fractionation.

The direct production of light olefins via Fischer-Tropsch-to-olefins concepts has attracted considerable academic interest, particularly with promoted iron-based catalysts or oxide–zeolite bifunctional systems [17,18]. Despite extensive research efforts, achieving high selectivity toward C_2–C_4 olefins while suppressing methane and heavy hydrocarbon formation remains challenging. An alternative approach involves the indirect production of light olefins through steam cracking of FT-derived naphtha fractions. FT-derived feeds are typically highly paraffinic, rich in linear hydrocarbons, and contain negligible amounts of aromatics, sulfur, nitrogen, and halogens. Such a composition favors ethylene formation through successive β-scission reactions during steam cracking [19–21].

Despite the industrial maturity of Fischer-Tropsch synthesis, comprehensive evaluations of FT-derived feedstocks as steam cracker feeds remain limited, with only a few studies reported in the literature [19–22]. In particular, more comprehensive assessments, including upgrading strategies, cracking performance, and steam cracker-level CO_2 intensity for FT-derived feedstocks, remain lacking. Addressing this gap is essential not only to quantify their technical performance but also to clarify their practical potential and the strategies needed to overcome the limitations of implementing CO_2-derived FT feedstocks within existing steam cracking infrastructure. To address these gaps, this study presents a systematic experimental investigation of CO_2-derived Fischer-Tropsch feedstocks for industrial steam cracking applications. The FT-derived feedstocks were synthesized at the VTT Technical Research Centre of Finland from CO_2 via Reverse Water-Gas Shift (RWGS) followed by Fischer-Tropsch synthesis and subsequent distillation and hydrotreatment, to tailor their boiling range and chemical stability. Comprehensive compositional characterization was performed using two-dimensional gas chromatography (GC × GC), coupled with various detectors. Feedstock performance was evaluated in a continuous bench-scale steam-cracking reactor operated under industrially relevant conditions and benchmarked against fossil naphtha at the Laboratory for Chemical Technology, Ghent University. Product yields, coke formation, and the CO_2 intensity of the steam cracking process were analyzed to determine the viability of CO_2-derived FT feedstocks as circular alternatives for light olefin production within existing petrochemical infrastructure.

1.1. Apparatus and experimental procedure

Fig. 1 illustrates the valorization of carbon dioxide feedstock together with green hydrogen into hydrocarbons via a tandem process based on Fischer-Tropsch synthesis. Because conventional Fischer-Tropsch catalysts exhibit limited activity for direct CO_2 hydrogenation, an intermediate conversion step is required. This is achieved via the reverse water–gas shift (RWGS) reaction, which generates CO upstream of the FT reactor. In this concept, an integrated catalytic partial oxidation (CPOX)/RWGS unit utilizes recycled C_1–C_4 FT hydrocarbons and unconverted gaseous species as additional feedstocks, together with oxygen. The resulting exothermic oxidation of H_2, CO, and C_1–C_4 hydrocarbons supplies heat directly to the endothermic RWGS reaction, enabling near-autothermal operation of the reactor. Simultaneously, recycling light FT products and unconverted reactants improves overall carbon utilization and process efficiency. Further details of the (CPOX)/RWGS and Fischer-Tropsch process used in this study can be found in Section A1 of the Supporting Information (SI).

The produced FT oil was then distilled and hydrotreated to obtain the upgraded feedstocks. Hydrotreatment was performed to remove oxygenates and olefins using a two-stage process with a 3% Pt/γ-Alumina catalyst in a bench-scale high-throughput reactor system. The catalyst was prepared at VTT via incipient wetness impregnation of commercial γ-alumina extrudates (Harshaw Chemie B.V., 1/16 in., BET surface area 200 $m^2 \cdot g^{-1}$) with an appropriate amount of $Pt(NO_3)_4$ solution (Johnson Matthey). The low-temperature hydrotreatment (160 °C, 50 bar) targeted the removal of olefins, while the high-temperature hydrotreatment (340 °C, 50 bar) targeted the removal of oxygenates. More detailed descriptions of the equipment and procedures can be found in the Materials and Methods section of the SI. For these trials, gases supplied by AGA Linde were used, including industrial-grade hydrogen (purity 5.0), helium (purity 5.6), air (purity 5.0), nitrogen (purity 5.0), and argon (purity 5.0). Distillation of the FT oil was performed using a Pilodist PD104HT unit. A 200°C cut point was applied to obtain a narrow-boiling-range FT naphtha fraction. As a result of FT synthesis and upgrading, three FT-derived feedstocks were obtained for evaluation in steam cracking. The first feedstock is the crude FT oil collected directly from the FT unit's cold trap (i.e., oil decanted from the FT product water). The second feedstock is hydrotreated (HDT) FT oil, a product of hydrotreating FT oil. The third feedstock is HDT FT naphtha, produced by sequential distillation and hydrotreatment of the FT oil. The hydrocarbon, heteroatom, and halogen compositions of the FT-derived feedstocks were investigated using advanced comprehensive two-dimensional gas chromatography (GC × GC) coupled with various detectors. The hydrocarbon composition was determined using GC × GC coupled to a flame ionization detector (FID). Nitrogen chemiluminescence (NCD) and sulfur chemiluminescence (SCD) detectors, connected to a flow-modulated GC × GC instrument (Agilent 8890 GC system), were used to analyze nitrogen- and sulfur-containing compounds, respectively. The oxygen- and chlorine-containing compounds were analyzed using GC × GC coupled with atomic emission detection (AED), while metal contaminants were quantified by inductively coupled plasma optical emission spectroscopy (ICP-OES). Details of the analytical methods and the corresponding limits of detection (LODs) are provided in the SI. The analytical procedures are described in Section A3, while the LODs for the GC × GC detectors and the ICP-OES analysis are summarized in Tables S15 and S17, respectively.

The steam cracking experiments were conducted using the bench-scale steam cracker (BSSC) at the Laboratory for Chemical Technology

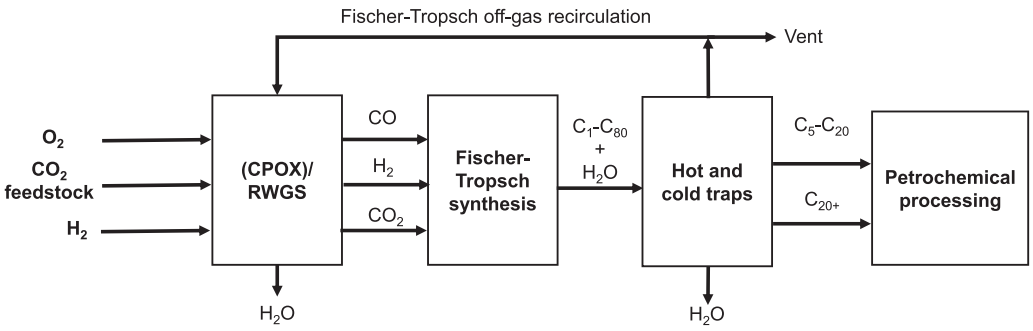


Fig. 1. Integrated pathways for valorization of CO_2-Derived feedstocks through CPOX, RWGS, and Fischer–Tropsch synthesis.

(LCT), Ghent University. The BSSC is designed for scale-down simulation of industrial steam cracker furnaces [23]. Detailed descriptions of the setup and operating procedures are available in previous studies [24–26]. A schematic representation is provided in Figure S4 in the SI. Steam cracking was performed at a liquid hydrocarbon flow rate of 150 g h^{-1} , a steam-to-hydrocarbon mass ratio of 0.5, and a coil outlet pressure of 1.7 bar. The coil inlet temperature was maintained at 550 °C, while three coil outlet temperatures (COTs) of 820, 850, and 880 °C were evaluated. The reactor effluent was analyzed on-line using a combination of a refinery gas analyzer (RGA), GC × GC-FID, and a light oxygenates analyzer (LOA), enabling comprehensive quantification of gaseous and liquid products. Product yields were determined using an overall mass-balance closure with an accuracy of ±5%. The coking tendency of the investigated feedstocks was then evaluated. Additional operating conditions are summarized in section A4 in the SI. Finally, a carbon footprint analysis was conducted to assess the impact of FT-derived feedstocks on the cracker-level CO_2 intensity of ethylene production; details are provided in Section A5 of the SI.

2. Results and discussion

2.1. Steam cracker feedstock analysis

The hydrocarbon compositions of the FT-derived feedstocks and the reference fossil naphtha, determined via GC × GC-FID, are summarized in Table 1. Additional compositional information is available in section B1 of the SI.

Table 1 summarizes the key characteristics of FT and fossil feedstocks, including hydrocarbon composition; initial, 50%, and final boiling points (IBP, 50% BP, FBP) determined by GC × GC-FID analysis. Based on their boiling point distributions, FT oil (14–371°C) and HDT FT oil (14–371 °C) are categorized as straight-run distillates. HDT FT naphtha (14–203 °C) falls within the wide-cut naphtha range, whereas the reference fossil naphtha (30–182 °C) aligns with typical full-range naphtha specifications. The fossil naphtha exhibits a carbon-number distribution from C_5 to C_{10}, with iso-paraffins as the dominant group (44.6 wt%), followed by n-paraffins (26.3 wt%) and naphthenes (20.9 wt%). Monoaromatics account for a minor fraction (8.2 wt%), while olefins, diolefins, and oxygenates were not detected. The FT oil has a broader carbon-number distribution, ranging from C_5 to C_{23}. The FT oil consists primarily of linear hydrocarbons, including 75.8 wt% n-paraffins, 11.4 wt% primary alcohols, and 9.7 wt% α-olefins (See Table 1). As shown in the GC × GC-FID plots in Fig. 2, only minor amounts of branched species were detected, comprising 1.2 wt% iso-paraffins, 1.6 wt% iso-olefins, and 0.3 wt% secondary alcohols, predominantly 2-alcohols. No diolefins, naphthenes, or aromatics were observed.

Table 1
The hydrocarbon composition of the Fischer-Tropsch-derived feedstocks and the fossil naphtha was analyzed using GC × GC-FID.

Feedstock	FT oil	HDT FT oil	HDT FT naphtha	Fossil naphtha
IBP [°C]	14	14	14	30
50% BP [°C]	183	183	136	81
FBP [°C]	371	371	203	182
Carbon number range	$C_5 - C_{23}$	$C_5 - C_{23}$	$C_5 - C_{12}$	$C_5 - C_{10}$
Hydrocarbon groups [wt%]:				
Paraffins	75.8	98.0	98.5	26.3
Iso-paraffins	1.2	1.7	1.5	44.6
α-Olefins	9.7	< 0.01	< 0.01	< 0.01
Iso-olefins	1.6	< 0.01	< 0.01	< 0.01
Naphthenes	< 0.01	< 0.01	< 0.01	20.9
Monoaromatics	< 0.01	< 0.01	< 0.01	8.2
Paraffinic oxygenates	11.4	0.3	< 0.01	< 0.01
Isoparaffinic oxygenates	0.3	< 0.1	< 0.01	< 0.01

Olefins and oxygenates in the FT oil, measured by the GC × GC-FID analysis, amount to 11.3 wt% and 11.7 wt%, respectively, both substantially exceeding the industrial thresholds for steam crackers (2 wt% for olefins and 0.01 wt% for oxygen) [26–28]. The relatively high amount of oxygenates in the FT oil, 11.7 wt%, was unexpected. Typically, low-temperature cobalt-based Fischer-Tropsch catalysts, especially under industrial conditions, produce mostly linear hydrocarbons while the share of alcohols is about 1.5 wt% [29]. However, high selectivity to long-chain alcohols, as in the current case, has also been reported [30–36]. One possible explanation is that the cobalt was not fully reduced, as higher temperatures may be needed to reduce well-dispersed cobalt species [15]. Previous studies have associated the enhanced formation of heavier alcohols with the presence of non-reduced Co^{2+} species, which may act as sites for non-dissociative carbon monoxide adsorption and thereby facilitate chain termination toward primary alcohols [36]. The composition of the gas entering the FT reactor may also influence the catalyst reduction state. Unlike the industrially operated FT reactor, the FT reactor used in this study has a significant amount of CO_2 remaining unconverted in the FT feed gas after the RWGS step (see Figure S2 in the SI). Literature reports indicate that CO_2 can influence both the rate of catalytic hydrogenation of CO and the product distribution and may act as a mild oxidizing agent toward reduced cobalt, thereby favoring the presence of partially oxidized Co^{2+} species [37–39]. Accordingly, the residual CO_2 in the FT feed could have contributed to the observed alcohol formation, although this relationship was not directly verified for the catalyst under the conditions investigated here. Recent research on integrated RWGS-FT systems is increasingly focused on tighter coupling of the two processes by minimizing intermediate syngas conditioning, accommodating residual CO2 and H2O in the FT feed, and optimizing the overall process rather than the individual RWGS and FT steps [40–43]. Although detailed optimization of RWGS-FT integration is beyond the scope of the present work, these studies provide relevant context for the composition of the gas entering the FT reactor in the investigated process configuration.

The presence of these oxygenates and olefins in the feedstock poses challenges for steam-cracking compatibility, as they act as precursors to dienes and aromatics, which are associated with increased fouling and coke formation. Oxygenates are known to cause fouling and corrosion in

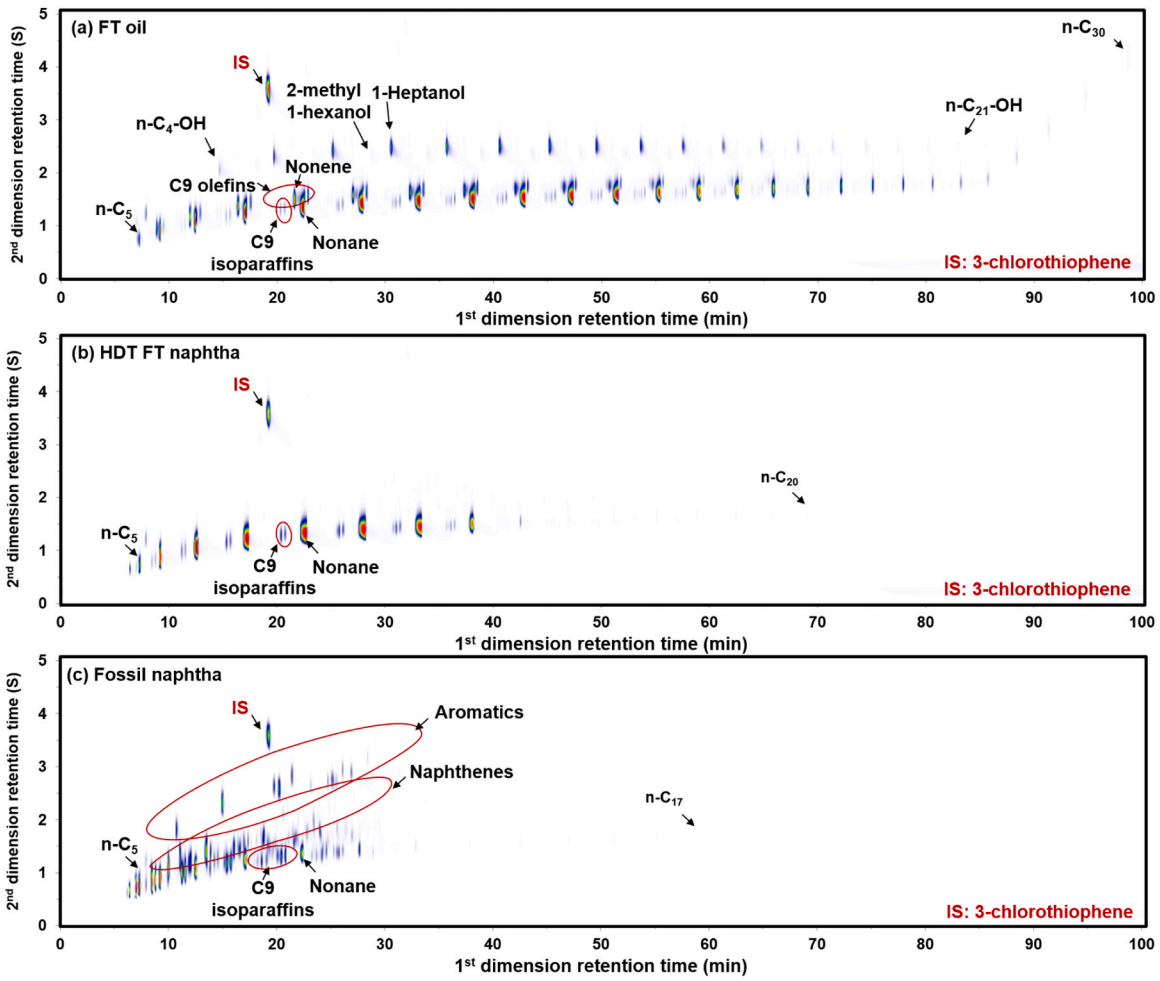


Fig. 2. GC × GC-FID chromatograms of the Fischer-Tropsch derived feedstocks: (a) crude oil collected from the cold trap (FT oil), (b) after hydrotreatment and distillation (HDT FT naphtha), and (c) fossil naphtha.

downstream separation units [24,44–46]. The presence of oxygenates in the feed can generate problematic by-products during steam cracking, such as CO, methanol, formaldehyde, elemental oxygen, and organic acids, which promote corrosion, catalyst deactivation, and the formation of off-spec gas streams [46,47]. For instance, organic acids may accumulate in quench water systems, accelerating equipment degradation, while elemental oxygen can react with butadiene species to form gums, exacerbating fouling [46,48,49]. Although carbon monoxide (CO), formed from oxygenate decomposition, is not a primary fouling agent, it can still influence product distribution and act as a poison for the downstream catalysts [46,50]. Hydrotreatment resolved these issues associated with oxygenates and olefins in the FT oil by converting them into saturated hydrocarbons. The produced HDT FT oil contained 98.0 wt% n-paraffins and 1.7 wt% iso-paraffins, with no detectable naphthenic or aromatic species. The feedstocks were further evaluated for heteroatomic contaminants, including nitrogen, sulfur, and chlorine; none were detected, indicating concentrations below the analytical detection limits (see the contaminants analysis in section B1 of the SI). The syngas supplied to Fischer-Tropsch synthesis is typically low in contaminants because the severe conditions of catalytic partial oxidation suppress the formation of heavy byproducts and promote phase separation. In the CO_2-derived carbon route, captured CO_2 serves as the primary carbon source and is converted via the RWGS reaction to generate a well-defined CO/H_2 mixture. The FT-derived feedstocks had low total metal concentrations, ranging from 7 to 14 ppm (see Table S16 in the SI), reflecting the limited introduction of contaminant-bearing species during feedstock production.

2.2. Steam cracking performance

To evaluate the steam-cracking performance of FT-derived feedstocks, product yields were assessed at three severities, defined by coil outlet temperatures (COTs) of 820°C, 850°C, and 880°C (see detailed temperature profiles in Table S4 of the SI). This range reflects typical operating conditions for naphtha cracking [51] and allows for direct comparison with other circular feedstocks previously tested under the same setup [26,28,52].

Fig. 3 presents GC × GC chromatograms from on-line sampling of the reactor effluent during cracking at a COT of 850 °C. These chromatograms provide contour plots of the resulting hydrocarbon products. For downstream processing considerations, the products are generally classified into three categories: C_{4-} components (light olefins and alkanes), pyrolysis gasoline (PyGas, C_5–C_9; e.g., benzene, toluene, xylenes), and pyrolysis fuel oil (PFO, C_{10+}; e.g., naphthalene, phenanthrene). While light olefins, namely ethylene, are the primary target products, PyGas and PFO are inevitable by-products, especially pronounced during the cracking of liquid feedstocks, such as naphtha and gas oil, compared to gaseous feeds, such as ethane, propane, and butane [51,53]. Although complete suppression of these by-products is not feasible, cracking conditions are typically optimized to minimize the formation of heavier aromatic-rich streams and to avoid over-cracking. Severe cracking conditions promote secondary reactions, aromatization, and condensation, in which valuable light olefins are further converted into heavier aromatics and coke, thereby reducing ethylene yield, increasing energy demand, and shortening furnace run length.

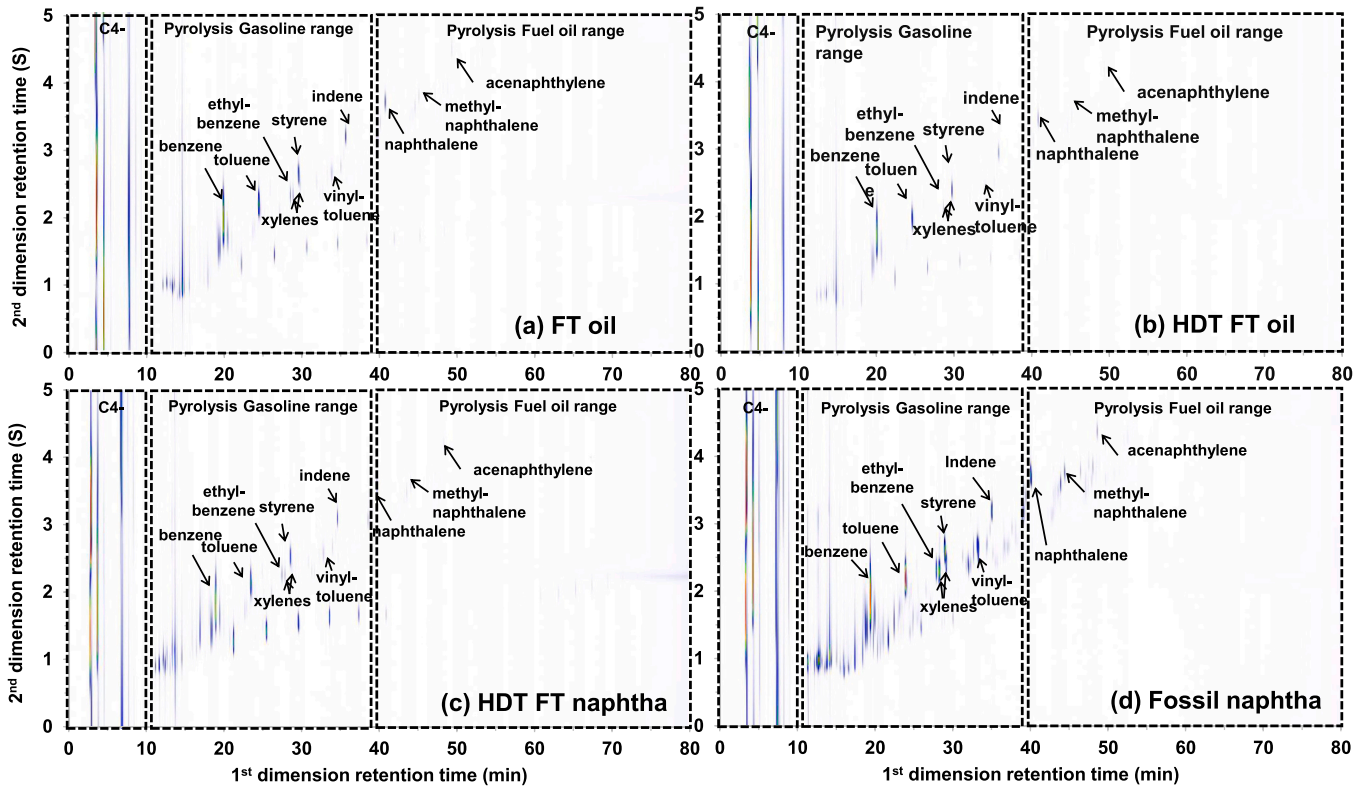


Fig. 3. GC × GC–FID chromatograms for the on-line sampled reactor effluents from cracking at COT of 850 °C (a) FT oil; (b) HDT FT oil; (c) HDT FT naphtha; (d) Fossil naphtha.

Fig. 4 presents the yields of key steam cracking products, including methane, light olefins (ethylene, propylene, 1,3-butadiene), pyrolysis gasoline (PyGas), and pyrolysis fuel oil (PFO), as a function of coil outlet temperature (COT) for FT-derived feedstocks and reference fossil naphtha. As also detailed in Table 2, a clear difference in light olefin yields is observed between FT-derived and fossil-based feedstocks, primarily due to significantly higher ethylene production from FT-derived feedstocks. At a COT of 850 °C, for example, ethylene yields reached 37.3 wt% for FT oil, 40.3 wt% for hydrotreated (HDT) FT oil, and 40.8 wt% for HDT FT naphtha, compared to only 26.2 wt% for fossil naphtha. These higher ethylene yields from FT-derived feedstocks are primarily due to their high n-paraffin content. It is well established that linear hydrocarbons favor free-radical cracking mechanisms, promoting ethylene formation through successive β-scission reactions [50,54]. Steam cracking proceeds via a free-radical chain mechanism involving radical initiation, hydrogen abstraction, β-scission, radical isomerization, hydrogen transfer, and termination. Cracking of linear n-paraffins generates alkyl radicals that preferentially undergo successive β-scission reactions, producing ethylene together with shorter alkyl radicals that continue propagating the radical chain mechanism. In contrast, radicals derived from iso-paraffins are more highly substituted and therefore more stable, promoting competing isomerization and hydrogen-transfer reactions before β-scission, which favors the formation of branched olefins and light gases. This mechanistic advantage is reflected in the lower propylene-to-ethylene (P/E) ratios observed: 0.42 for both FT oil and HDT FT oil, and 0.40 for HDT FT naphtha, compared to 0.57 for

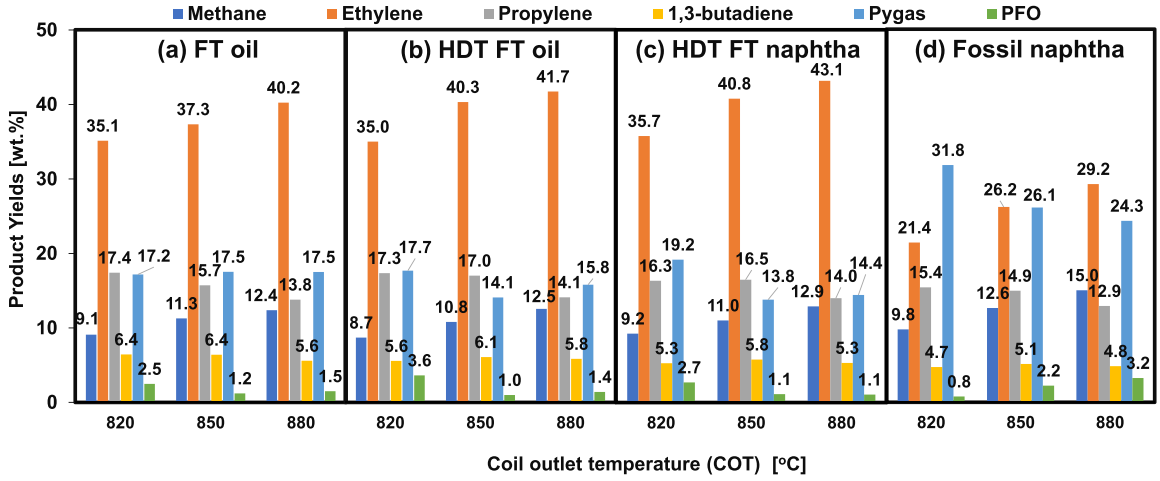


Fig. 4. The most important product yields as a function of the coil outlet temperature (COT) for FT-derived feedstocks: (a) FT oil, (b) HDT FT oil, (c) HDT FT naphtha versus (d) reference fossil naphtha.

Table 2
Summary of the most important product yields from steam cracking of Fischer-Tropsch-derived feedstocks and the fossil naphtha as a function of the coil outlet temperature (COT).

	FT oil			HDT FT Oil			HDT FT naphtha			Fossil naphtha		
COT [°C]	820	850	880	820	850	880	820	850	880	820	850	880
Total C_1-C_4 [wt%]	80.28	81.28	81.13	78.72	84.96	82.85	78.15	85.10	84.55	67.45	71.67	72.45
PyGas (C_5-C_9) [wt%]	17.19	17.51	17.38	17.56	14.15	15.71	19.13	13.78	14.39	31.79	26.12	24.33
PFO (C_{10+}) [wt%]	2.54	1.21	1.49	3.72	0.89	1.44	2.71	1.12	1.06	0.76	2.21	3.23
Propylene/Ethylene [-]	0.50	0.42	0.34	0.50	0.42	0.34	0.46	0.40	0.32	0.72	0.57	0.44
Propylene + Ethylene [wt%]	52.53	53.04	54.03	52.31	57.29	55.78	52.07	57.23	57.13	36.81	41.12	42.14
Concentration of important products in the reactor effluent [wt%]												
H_2	0.57	0.72	0.84	0.54	0.74	0.92	0.59	0.75	0.98	0.75	0.89	1.07
CO	0.66	0.87	0.94	0.04	0.05	0.07	0.04	0.04	0.06	0.09	0.12	0.16
Methane	9.09	11.28	12.37	8.68	10.79	12.55	9.24	11.01	12.90	9.77	12.63	15.01
Ethylene	35.12	37.33	40.24	34.97	40.29	41.69	35.75	40.76	43.15	21.40	26.18	29.25
Ethane	4.06	4.25	3.66	4.09	4.15	3.78	4.07	4.22	3.95	2.94	3.05	2.96
Propylene	17.41	15.71	13.80	17.34	17.00	14.09	16.32	16.47	13.98	15.40	14.94	12.89
1-butene	4.49	2.11	1.08	5.04	3.17	1.19	4.30	3.27	1.44	2.96	1.86	0.94
Iso-butene	0.22	0.22	0.17	0.20	0.22	0.19	0.21	0.22	0.19	2.87	2.37	1.65
1,3-butadiene	6.44	6.41	5.59	5.56	6.07	5.84	5.26	5.77	5.32	4.71	5.12	4.83
1-pentene	1.09	0.30	0.00	1.56	0.16	0.12	1.46	0.54	0.13	2.61	1.27	0.38
1,3-cyclopentadiene	1.89	2.56	2.80	1.54	2.58	2.60	0.76	1.67	2.36	1.40	1.88	1.94
Benzene	3.29	6.47	7.39	2.32	5.20	6.68	1.63	2.38	5.72	2.35	6.61	8.46
Toluene	0.92	1.60	1.75	0.71	1.11	1.51	0.45	0.76	1.27	3.14	3.81	4.30
Xylenes	0.12	0.17	0.19	0.06	0.07	0.15	0.04	0.08	0.16	1.25	1.43	1.71
Indene	0.12	0.27	0.45	0.08	0.23	0.38	0.06	0.13	0.33	0.09	0.35	0.57
Naphthalene	0.10	0.27	0.56	0.07	0.24	0.51	0.04	0.13	0.37	0.14	0.47	0.96
BTX	4.33	8.25	9.33	3.08	6.38	8.34	2.12	3.22	7.15	6.74	11.86	14.47

fossil naphtha at 850 °C. The reduced P/E ratio indicates greater ethylene selectivity in FT-derived feedstocks. Notably, despite the lower P/E ratio, propylene yields from FT feeds were still slightly higher than those from fossil naphtha. This suggests that the overall light olefin productivity is enhanced due to the predominance of linear paraffins in FT-derived feedstocks, which are more prone to undergo β-scission under steam cracking conditions.

The yield of isobutene, a branched olefin, was markedly higher for fossil naphtha (2.4 wt% at 850 °C) compared to FT-derived feedstocks (0.2 wt% across all FT-derived feedstocks at 850 °C), indicating a stronger propensity for branched olefin formation in the fossil feed. This difference appears to come at the expense of 1-butene, which was associated with slightly higher yields in FT-derived feedstocks**.** The high iso-paraffin (44.6 wt%) and naphthenic content (20.9 wt%) of fossil naphtha (see Table 1) promote secondary cracking pathways that favor branched olefin formation relative to linear-alkane-rich feedstocks. This increase in branched olefins yields is also accompanied by lower yields of ethylene and propylene and higher yields of light gases, particularly methane and hydrogen. The methane yield from steam cracking of the fossil naphtha at a COT of 850 °C resulted in 12.6 wt%, compared to 11.3 wt% for FT oil and 10.8 wt% for HDT FT oil under similar conditions. Feedstocks rich in iso-paraffins and naphthenes exhibit a greater tendency toward over-cracking, converting valuable light olefins into methane and hydrogen, and thereby reducing overall carbon efficiency [55,56].

FT-derived feedstocks, on the other hand, produced higher yields of light olefins than fossil naphtha. Their high n-paraffin content promotes β-scission and dehydrogenation during steam cracking, thereby enhancing the formation of light olefins and conjugated dienes, such as 1,3-butadiene. Previous studies have shown that linear alkanes crack more selectively into olefins and dienes than branched or cyclic hydrocarbons [50,57]. Dijkmans et al. reported that steam cracking of a hydro-deoxygenated paraffinic feedstock at 835 °C yielded 38.0 wt% ethylene, 20.0 wt% propylene, and 7.5 wt% 1,3-butadiene [57]. Under the same conditions, fossil naphtha produced lower yields: 27.2 wt%, 16.3 wt%, and 4.7 wt%, respectively. In contrast, feedstocks rich in iso-paraffins and naphthenes, such as those studied by De Bruycker et al., showed lower selectivity toward light olefins and dienes due to increased secondary reactions and enhanced aromatic formation [58,59]. These findings highlight the significant impact of feedstock structure on product distribution during steam cracking. The favorable light-olefin yields observed for the FT-derived feedstocks are consistent with previous studies on the steam cracking of FT-derived feedstocks, which demonstrated the superior performance of predominantly linear paraffinic FT feedstocks for light-olefin production, favoring higher ethylene yields and lower formation of heavier by-products compared with conventional fossil naphthas [19–21].

As shown in Fig. 4 and Table 2, steam cracking of FT oil and other FT-derived feedstocks produced significantly lower yields of pyrolysis gasoline (PyGas, C_5–C_9) compared to fossil naphtha. Compared with fossil naphtha, steam cracking of FT oil reduced the PyGas yield from 31.8 to 17.2 wt% at 820 °C (46% reduction), from 26.1 to 17.5 wt% at 850 °C (33% reduction), and from 24.3 to 17.4 wt% at 880 °C (29% reduction). This difference is primarily due to variations in the feedstock composition. Approximately 96 wt% of the fossil naphtha falls within the C_5–C_9 carbon range. At lower cracking temperatures (e.g., COT of 820 °C), a substantial fraction of the PyGas yield can therefore be attributed to unconverted feedstock components. In contrast, FT-derived feedstocks contain a higher proportion of C_{10+} hydrocarbons, which preferentially crack into lighter products rather than contribute to the PyGas range. Moreover, fossil naphtha produced significantly more C_6–C_9 aromatics, including benzene (C_6), toluene (C_7), and xylenes (C_8). For example, at 850 °C, the BTX yield reached 11.9 wt% for fossil naphtha, compared to 8.3 wt% for FT oil (Table 2). Two factors can explain this difference. First, fossil naphtha already contains notable amounts of aromatic species, which are relatively resistant to conversion under mild or moderate cracking conditions and therefore persist in the product slate (Table 1). Second, its high content of isoparaffinic compounds (44.6 wt%) and naphthenes (20.9 wt%) promotes in situ aromatic formation via dehydrogenation and reactions during steam cracking [58,60]. At a COT of 820 °C, FT oil produced a higher PFO yield than fossil naphtha, with yields of 2.54 and 0.76 wt%, respectively (see

Fig. 4). The higher PFO yield from FT oil is primarily attributed to the incomplete conversion of heavy C_{10+} components, as detailed in Section B2 of the SI. Increasing the COT to 850 °C reduced the PFO yield from FT oil from 2.54 to 1.21 wt%, indicating enhanced cracking of the heavier C_{10+} hydrocarbons. In contrast, the PFO yield from fossil naphtha increased from 0.76 to 2.21 and 3.23 wt% as the COT increased from 820 to 850 and 880 °C, respectively, reflecting intensified secondary reactions and polycyclic aromatic hydrocarbon (PAH) formation, with naphthalene becoming the dominant PAH at 880 °C. Nevertheless, the PFO produced from the FT-derived feedstocks contained considerably lower PAH concentrations. This observation is consistent with the lower contents of branched and cyclic hydrocarbons in the FT-derived feedstocks (See Table 1), which are important precursors for PAH formation [26]. Notably, steam cracking of FT oil yielded higher CO yields, consistent with the feedstock composition. FT oil contained approximately 11.7 wt% alcohols, corresponding to around 0.97 wt% oxygen, which contributed to elevated CO formation (see Table 2). To investigate the fate of these oxygenates, additional analysis was conducted using an on-line LOA to detect expected light oxygenates such as methanol and formaldehyde. However, none of the compounds were detected, suggesting that the oxygen from the alcohols was primarily converted to CO and possibly water. Previous studies have shown that the presence of oxygenates in steam cracking feedstocks promotes the formation of CO and CO_2, even at relatively low temperatures (e.g., 800 °C) [24,45]. Harper et al. reported that pyrolysis of n-butanol at ~ 650 °C produces intermediate oxygenates, including formaldehyde, acetaldehyde, butanal, and methanol [25]. At higher temperatures (>800 °C), these intermediates undergo further cracking, resulting in CO as the dominant oxygen-containing product. Similar behavior has been reported during the steam cracking of bio-based feedstocks, including hydrotreated tall oil fatty acids (HDO-TOFA) [50], hydrotreated distilled tall oil (HDO-DTO) [50], rapeseed oil methyl ester (RME) [24], hydrotreated crude tall oil (HDO-CTO) [58], as well as methyl decanoate as a model fatty acid methyl ester (FAME) [45]. In all cases, cracking at industrially relevant temperatures (e.g., >800 °C) consistently led to increased CO formation and, in some instances, CO_2 formation, depending on the feedstock composition. Overall, the fate of oxygenates during steam cracking depends on the severity of cracking and the intrinsic reactivity of the oxygen-containing functional groups. A more detailed investigation examining the effects of oxygen functional groups, carbon chain length, oxygenate concentration, and temperature would provide further insight, but it falls beyond the scope of this study.

The impact of hydrotreatment on FT oil was assessed by comparing untreated and hydrotreated feedstocks. Hydrotreatment markedly improved cracking performance, enhancing light-olefin selectivity while reducing undesired byproducts. The combined ethylene and propylene yield increased from 53.04 wt% for untreated FT oil to 57.29 wt% at 850 °C after hydrotreatment, accompanied by a substantial reduction in CO formation, from 0.66 to 0.94 wt% to 0.04–0.07 wt%, confirming effective oxygenate removal. In addition, hydrotreatment suppressed the formation of heavier products, including PFO and BTX aromatics, consistent with reduced availability of precursors for secondary reactions [50,59]. Among the FT-derived feedstocks, HDT FT naphtha exhibited the highest ethylene selectivity and the lowest heavy byproduct formation, attributable to its lighter, narrower boiling-range composition.

The second aspect in evaluating the steam-cracking performance of FT-derived feedstocks is their coking tendency. This parameter is critical to the economic operation of industrial steam crackers, as excessive coke formation shortens run lengths and necessitates more frequent shutdowns for decoking. The run-length, defined as the operating time between decoking cycles, is a key indicator of feedstock suitability. In this study, the measured coke deposition reflects the amount of coke formed within the steam cracker's radiant coils.

Fig. 5 presents a graphical summary of radiant coil coke formation for the tested FT-derived feedstocks. Among the FT-derived feedstocks,

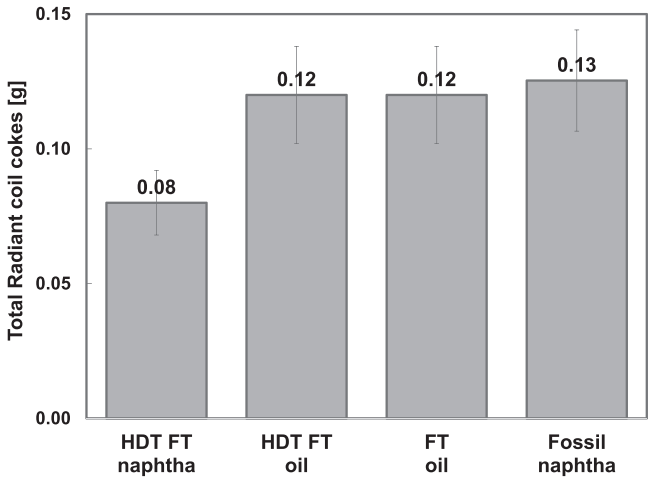


Fig. 5. Overview of radiant coil coke formation during a straight 6-hour steam cracking run at COT of 850 °C for different feedstocks.

HDT FT naphtha exhibited the lowest coke formation, with a total accumulation of 0.08 g. FT oil and HDT FT oil showed similar coke levels of 0.12 g. The coke quantified in this study, however, was limited to deposits formed within the radiant coil of the bench-scale steam cracker, while coke and fouling occurring in the convection and downstream sections were not evaluated. In particular, coke originating from the unsaturated compounds present in the FT-derived feedstocks is expected to form predominantly in these colder sections rather than within the radiant coil, as previously reported [61]. Consequently, although the present bench-scale experiments provide reliable comparative data under industrially relevant cracking conditions, a comprehensive assessment of long-term coke formation and fouling under industrially representative operating conditions remains necessary. Such investigations will be carried out using the dedicated Fouling Assessment SeTup (FAST) unit developed in our laboratory, which is specifically designed to evaluate fouling and coke formation in the reactor, convection section, and transfer line exchanger under industrially relevant conditions [62,63]. In industrial scenarios, FT-derived feedstocks are expected to be blended with fossil naphtha, which would likely dilute olefinic and oxygenated species and reduce fouling risks in the convection section and transfer line exchanger (TLE). Given the low contaminant levels in the FT-derived feedstocks, including metals such as Fe and Ni, known to catalyze coke formation [26,51], along with their narrow boiling ranges and lack of naphthenes and aromatics, radiant coil coke formation is not a significant concern.

2.3. FT-derived feedstocks as feeds for steam crackers: Potential and limitations

Despite their strong sustainability profile and favorable steam cracking characteristics, particularly their paraffinic composition and low impurity levels, FT-derived feedstocks have not yet been widely implemented in industrial steam crackers. This section outlines the main opportunities and challenges associated with their use in light olefin production, including feedstock contamination, operational constraints, integration approaches, and economic and energy considerations. Table 3 summarizes the key parameters relevant for assessing FT-derived feedstocks in this context. In general, even without further treatment, FT-derived feedstocks are inherently clean, exhibiting very low concentrations of halogens, sulfur, and nitrogen, thereby minimizing the risks of corrosion and downstream catalyst deactivation. The trace metal content observed in this study is more likely attributable to catalyst leaching, laboratory equipment, or handling procedures rather than to the intrinsic nature of FT-derived materials. Consequently, metal contamination is not considered a major concern for their application as

Table 3
Key Parameters for evaluating FT-derived feedstocks as feeds for Steam Crackers (Adapted from [47]).

Parameter	Related issue	Possible contamination source in the FT synthesis and upgrading	Consideration of operating limits	FT oil	HDT FT oil	HDT FT naphtha
H/C [Mol·mol^{-1}]	-	-	H/C > 1.5	2.18	2.20	2.25
Olefins [wt%]	• Coking • Fouling	Formed as Fischer-Tropsch (FT) synthesis by-products	< 2.0	11.3	< LOD	< LOD
Nitrogen [mg·kg^{-1}]	• Corrosion [ammonia chloride (NH_4Cl)] • Operational instabilities (process water) • Catalyst deactivation	No Potential source	Feed-dependent indication: Naphtha < 100 Gasoil < 2000	< 100	< 100	< 100
Oxygen [mg·kg^{-1}]	• Increased fouling • Hydrogenation catalysts deactivation • Product yields	Formed as Fischer-Tropsch (FT) synthesis by-products	< 100 (as organic oxygen). No hard limit, depending on the type of oxygen components and cracker setup	9700	< 100	< 100
Sulfur [mg·kg^{-1}]	Lower concern	No Potential source	< 500	< 10	< 10	< 10
Cl and other halogens [mg·kg^{-1}]	• Corrosion • Potential for deposits • Product contamination • Catalyst poisoning	No Potential source	Cl and other halogens (e.g., F, Br): < 1.0–5.0	< 1.0	< 1.0	< 1.0
Si [mg·kg^{-1}]	Fouling and catalyst poisoning	No Potential source	Hard limit for Si: < 0.5–1.0	< 0.5	< 0.5	< 0.5
Alkali/salts [Na, calcium (Ca), magnesium, among others] [μg·kg^{-1}]	• Corrosion (Na: Hot corrosion of coils) • Coking • Fouling • Catalyst deactivation	Metals leaching from catalysts and process equipment	Na: < 125 (Hard limit) Ca: 500	1270 1370	4390 2420	440 600
Transition and heavy metals (e.g., Fe, Pb, V) [μg·kg^{-1}]	• Corrosion • Coking • Fouling • Catalyst poisoning		Al: -	2670	5180	1250
Total metals [μg·kg^{-1}]	-	-	Total metal < 2000	6970	14,360	8070
Final boiling point [°C]	Evaporation of feed must be ensured	-	Final boiling point < 580 (furnace type dependent)	371	371	203
Density [g·ml^{-1}]	-	-	< 0.9	0.74	0.74	0.71
Pour point [°C]	-	-	< -5		-	-

steam cracker feedstocks.

Olefins and oxygenates in FT-derived feedstocks, however, require careful attention, as they are present in considerable quantities in the FT oil (See Fig. 6). Blending with fossil naphtha is the most practical strategy to mitigate the olefin and oxygenates content of crude FT-derived feeds, as illustrated in Fig. 6. With 5 wt% FT oil blending, the total olefin content in the feedstock is reduced below the typical industrial threshold of 2 wt%. However, the oxygenates still do not meet the industrial threshold, even at 2.5 wt% blending. Hydrotreatment, as demonstrated in this study, is required to effectively eliminate oxygen and ensure compliance with industrial steam cracker specifications.

Compared to crude FT oil, hydrotreatment of FT oil allows higher proportions in steam cracker feed blends, potentially enabling the use of pure HDT FT oil, subject to production scale and economic viability. However, implementing hydrotreatment introduces additional hydrogen demand and energy consumption, thereby increasing the overall carbon footprint of FT-derived feedstocks. For this reason, the hydrotreatment severity, and consequently the hydrogen demand, need to be tailored to the targeted FT-oil blending ratio, which is governed by the intended application and the availability of feedstock for steam cracking. As illustrated in Fig. 6, the targeted FT-oil blending ratio determines the degree of oxygen removal required to limit the final blend's oxygen content to the maximum allowable level of 100 ppm. For example, oxygen removal of approximately 96%, 79%, and 59% is required to achieve oxygen contents of 400, 2000, and 4000 ppm, respectively, in the hydrotreated FT oil. These correspond to FT-oil blending ratios of 25, 5, and 2.5 wt%, while maintaining the maximum allowable oxygen content of 100 ppm in the final blend. Based on the experimental operating conditions and an elemental mass balance, as detailed in the SI (Section A2), the net hydrogen consumption for complete hydrotreatment of the FT-oil was estimated to be approximately 0.34 kg H_2 per 100 kg of FT oil. Although approximately 2.43 kg H_2 per 100 kg of FT oil is supplied to the reactor to maintain a sufficiently high hydrogen partial pressure, only about 14% of the supplied hydrogen is consumed by the hydrotreatment reactions. In industrial hydrotreatment units, the remaining hydrogen is routinely separated from the reactor effluent, purified, compressed, and recycled, resulting in a substantially lower net requirement for fresh hydrogen than the total hydrogen feed. Nevertheless, the FT oil investigated in this work contained only 0.97 wt% oxygen and 11.3 wt% olefins. Consequently, the hydrogen demand associated with complete hydrodeoxygenation and olefin hydrogenation was relatively low compared with more unsaturated feedstocks. For example, mixed plastic waste (MPW) pyrolysis oils typically contain more than 40 wt% olefins, making olefin hydrogenation a major contributor to the overall hydrogen demand during hydrotreatment. While the hydrogen demand associated with downstream upgrading can be optimized, as demonstrated in the previous paragraph. The hydrogen required for the RWGS reaction, which accounts for most of the hydrogen penalty, is inherent to the CO_2 conversion process and cannot be substantially reduced without compromising syngas production. Therefore, hydrogen production remains one of the principal energy challenges associated with industrial CO_2 utilization pathways. Although green hydrogen enables the near-carbon-neutral conversion of captured CO_2 into hydrocarbons, its production via water electrolysis requires substantial electrical energy and entails additional infrastructure requirements, including access to low-carbon electricity, a reliable water supply, and facilities for hydrogen production, transport, storage, and distribution. On the other hand, integration of hydrogen recovery and reuse within the refinery, for example by recovering hydrogen generated during steam cracking, could further improve the economic viability and environmental performance of the overall process. Therefore, comprehensive plant-wide

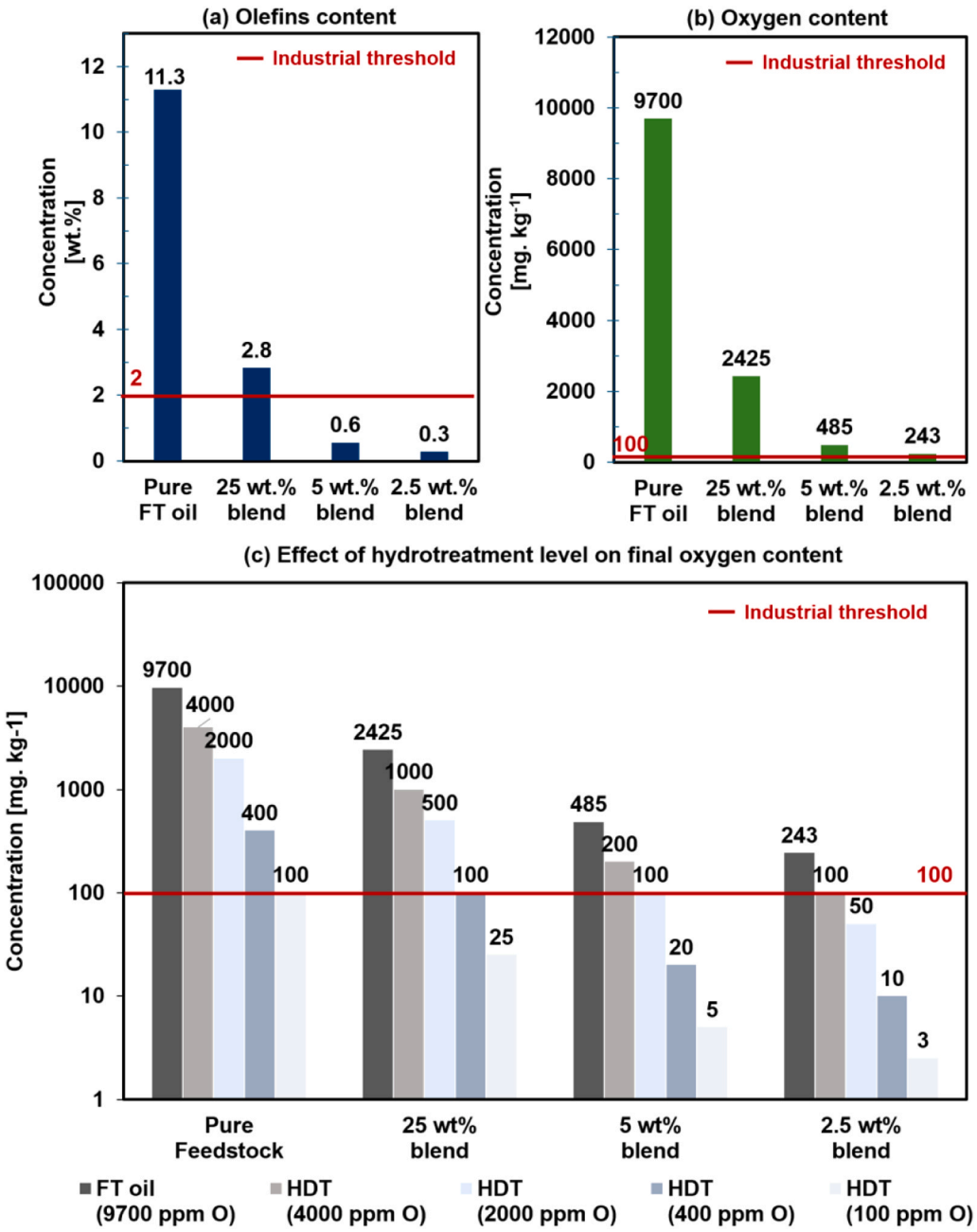


Fig. 6. Effect of blending FT oil with fossil naphtha on compliance with industrial steam cracker feedstock specifications: (a) olefin content, (b) oxygen content, (c) Effect of hydrotreatment level on final oxygen content, based on industrial threshold values reported in [26–28].

hydrogen integration analysis, including hydrogen recovery, purification, recycle, and utilization across the RWGS, hydrotreatment, and steam cracking units, is an important direction for future research. In conclusion, the economic, energetic, and environmental trade-offs of FT-derived feedstocks must be carefully evaluated when assessing upgrading scenarios and determining the most sustainable integration strategy.

The carbon intensity of steam cracking is primarily determined by furnace fuel combustion, which accounts for over 80% of the process's Scope 1 emissions [64]. Consequently, maximizing ethylene yield is critical to reducing fuel-derived CO_2 per ton of product. A comparative carbon footprint assessment indicates that raw FT oil reduces CO_2 emissions by 22% relative to fossil naphtha (Fig. 7). This performance is attributed to a paraffin-rich, aromatics-free composition that favors β-scission pathways, thereby maximizing ethylene selectivity. The oxygenated compounds present in the FT-derived stream generate CO during cracking. These oxygenate contaminants need to be removed by hydrotreatment. Nevertheless, the additional energy and hydrogen requirements associated with fractionation and hydrotreatment, together with only a limited improvement in CO_2 savings of approximately 7% compared with untreated FT oil, suggest a reduced overall environmental advantage for this upgrading step.

FT-derived feedstocks could serve as quality enhancers in steam cracking feedstock pools, facilitating the co-processing of lower-quality circular streams (Fig. 8). As shown in the different blending scenarios, recycling waste streams with a low hydrogen-to-carbon (H/C) ratio, such as the mixed-plastic pyrolysis oil evaluated in this study, typically incurs a carbon penalty due to low ethylene selectivity (Scenarios 2–4). This effect arises because hydrogen-deficient feedstocks exhibit lower ethylene selectivity and greater formation of aromatic-rich by-products, requiring more feedstock and furnace energy per unit of ethylene

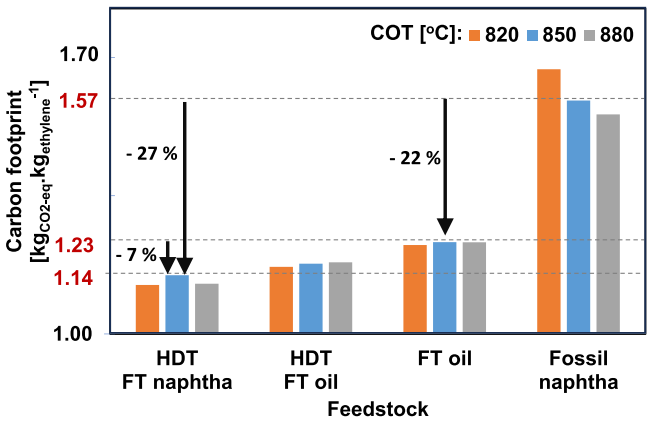


Fig. 7. Comparisons of the carbon footprint (expressed in $kg_{CO2\text{-}eq}.kg^{-1}_{ethylene}$) for ethylene synthesis via steam cracking of: HDT FT naphtha, HDT FT oil, FT oil, and Fossil naphtha.

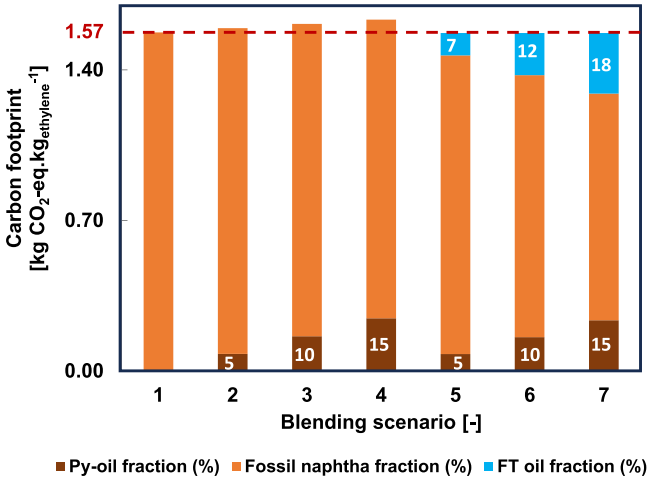


Fig. 8. Effect of integrating FT oil into pyrolysis oil and fossil naphtha blending scenarios on the CO_2 footprint of ethylene production (CO_2-eq per kg ethylene) at a COT of 850 °C.

produced. However, the addition of paraffinic FT oil acts as a chemical counterbalance. By blending FT oil with this hydrogen-deficient stream, operators can compensate for the low H/C ratio, thereby favoring β-scission over aromatic condensation. Notably, Scenario 7 demonstrates that up to 15% of a low-quality py-oil can be co-processed while maintaining a carbon footprint similar to the fossil naphtha baseline (red dotted line), provided it is balanced with 18% FT oil. This finding suggests that FT-derived feedstocks serve as strategic blending agents that unlock the processing of complex circular streams without compromising furnace run lengths or decarbonization targets. While this carbon footprint analysis focuses on the steam cracking process and excludes upstream production steps, it provides crucial data for refining such assessments. By establishing a preliminary carbon footprint based on specific yield distributions and process simulations, this study offers a detailed cracker-level analysis. These preliminary findings could serve as a foundation for more integrated, experimentally grounded techno-economic evaluations, particularly regarding trade-offs between feedstock quality and processing intensity (e.g., the impact of hydrotreatment).

3. Conclusions and outlook

This study presents a systematic experimental evaluation of CO_2-derived Fischer-Tropsch (FT) feedstocks as alternatives to steam crackers for light olefin production. Crude FT oil, hydrotreated FT oil, and hydrotreated FT naphtha were characterized and benchmarked against fossil naphtha. The FT-derived feedstocks were highly paraffinic and contained negligible aromatics, naphthenes, and heteroatomic contaminants, confirming their suitability for steam cracking. However, crude FT oil contained elevated levels of olefins and oxygenates, exceeding the respective industrial thresholds. Blending 5 wt% of FT oil with fossil naphtha can reduce this olefin content to compliant levels, while hydrotreatment is required to reduce oxygenate content. FT-derived feedstocks exhibited enhanced cracking performance, yielding higher ethylene and lower pyrolysis gasoline and pyrolysis fuel oil formation, with hydrotreated FT naphtha performing best due to its optimized boiling range. The increased ethylene yields resulted in lower CO_2 intensity at the cracker level than those from fossil-derived naphtha. Nevertheless, the additional hydrogen requirement and higher energy consumption associated with upgrading diminish the overall environmental advantage, underscoring a trade-off between feedstock quality and process sustainability. Fischer–Tropsch (FT)-derived feedstocks also offer promise as blending components in circular systems, serving as hydrogen-rich balancing streams that facilitate the co-processing of hydrogen-deficient inputs, such as plastic pyrolysis oils. In summary, CO_2-derived FT feedstocks represent clean, high-performance alternatives that can reduce dependence on fossil resources while enabling the integration of lower-quality circular carbon streams into existing steam-cracking infrastructure. Future research should prioritize techno-economic and life-cycle analyses, along with strategies for large-scale industrial implementation.

Nomenclature

Abbreviation / Symbol	Definition
CCU	Carbon Capture and Utilization
CPOX	Catalytic Partial Oxidation
RWGS	Reverse Water-Gas Shift reaction
COT	Coil Outlet Temperature (°C)
CIT	Coil Inlet Temperature (°C)
COP	Coil Outlet Pressure (bar)
FT	Fischer-Tropsch
FT oil	Crude FT oil collected after FT synthesis
HDT	Hydrotreatment or hydrotreated
HDT FT oil	Hydrotreated Fischer-Tropsch oil
HDT FT naphtha	Distilled and hydrotreated FT naphtha
FT-derived feedstocks	FT oil, HDT FT oil, and HDT FT naphtha
GC × GC	Comprehensive Two-Dimensional Gas Chromatography
FID	Flame Ionization Detector
SCD	Sulfur Chemiluminescence Detector
NCD	Nitrogen Chemiluminescence Detector
AED	Atomic Emission Detector
ICP-OES	Inductively Coupled Plasma – Optical Emission Spectroscopy
IBP	Initial Boiling Point (°C)
FBP	Final Boiling Point (°C)
P/E	Propylene-to-Ethylene yield ratio
PyGas	Pyrolysis Gasoline (C_5–C_9 fraction)
PFO	Pyrolysis Fuel Oil (C_{10}^+ fraction)
PAH	Polycyclic Aromatic Hydrocarbons
LOA	Light Oxygenates Analyzer
BSSC	Bench-Scale Steam Cracker

CRediT authorship contribution statement

Anas Jamil Abdulrahman: Conceptualization, Data curation, Investigation, Methodology, Visualization, Writing – original draft, Writing – review & editing. **Niko Heikkinen:** Conceptualization, Funding acquisition, Investigation, Methodology, Project administration, Writing – review & editing. **Miia Nevander:** Investigation, Writing – review & editing. **Miloš Auersvald:** Investigation, Methodology, Writing – review & editing. **Sphurti Prakash Kulkarni:** Investigation,

Methodology, Writing – review & editing. **Oleksii Mynko:** Investigation, Methodology, Writing – review & editing. **Behzad Parvizi:** Investigation, Methodology. **Daniël Withoeck:** Investigation, Methodology. **Marco Huotari:** Investigation. **Juha Lehtonen:** Funding acquisition, Project administration, Writing – review & editing. **Christian Frilund:** Investigation, Methodology, Writing – review & editing. **Matti Reinikainen:** Writing – review & editing. **Eveliina Mäkelä:** Investigation, Methodology, Writing – review & editing. **Marvin Kusenberg:** Investigation, Methodology, Writing – review & editing. **Kevin M. Van Geem:** Conceptualization, Funding acquisition, Project administration, Supervision, Writing – review & editing.

Declaration of Competing Interest

The authors declare that they have no known competing financial interests or personal relationships that could have appeared to influence the work reported in this paper.

Acknowledgments

This research was funded by the Business Finland Forest CUMP project (Dnro 2158/31/2022). This research has also received funding from the European Union's Horizon Europe Research and Innovation Programme (HORIZON-CL4–2021-TWIN-TRANSITION-01, Grant Agreement No. 101058412) and the European Research Council Programme (ERC, Grant Agreement No. 101142065). Marvin Kusenberg acknowledges financial support from the Fund for Scientific Research Flanders (FWO) through the postdoctoral fellowship grant 12ANG24N.

Appendix A. Supporting information

Supplementary data associated with this article can be found in the online version at doi:10.1016/j.jcou.2026.103555.

Data availability

Data will be made available on request.

References

[1] I.P.o.C.C. IPCC, in: H. Lee, J. Romero (Eds.), Climate Change 2023: Synthesis Report. Contribution of Working Groups I, II and III to the Sixth Assessment Report of the Intergovernmental Panel on Climate Change, Intergovernmental Panel on Climate Change IPCC, Geneva, Switzerland, 2023, p. 45.
[2] I.E.A. IEA, Energy Efficiency 2025, International Energy Agency IEA, Paris, 2025.
[3] I.E.A. IEA, Policy Toolbox for Industrial Decarbonisation, International Energy Agency (IEA), Paris, 2025.
[4] I.R.E.A. IRENA, Decarbonising hard-to-abate sectors with renewables: Perspectives for the G7, International Renewable Energy Agency, Abu Dhabi, 2024.
[5] O. Mynko, M. Bonheure, I. Amghizar, D.J. Brown, L. Chen, G.B. Marin, R. Freitas de Alvarenga, D. Civancik Uslu, J. Dewulf, K.M. Van Geem, Electrification of steam cracking as a pathway to reduce the impact of the petrochemical industry on climate change, J. Clean. Prod. 427 (2023).
[6] K.M. Van Geem, V.V. Galvita, G.B. Marin, Making chemicals with electricity, Science 364 (6442) (2019) 734–735.
[7] R. Cuéllar-Franca, P. García-Gutiérrez, I. Dimitriou, R.H. Elder, R.W.K. Allen, A. Azapagic, Utilising carbon dioxide for transport fuels: The economic and environmental sustainability of different Fischer-Tropsch process designs, Appl. Energy 253 (2019) 113560.
[8] G. Tweddle, L. Krause, P. Ruiz, A. Raschka, A. Özgen, N. Hark, M. Caru, Alternative Naphtha – Replacing Fossil-Based Feedstocks in Refineries and Naphtha Crackers: Technologies and Market, Status and Outlook, nova-Institute (2024).
[9] I.E.A. IEA, Global energy review, IEA, Paris, 2021. https://www.iea.org/reports/global-energy-review-2021, 2021.
[10] Y. Cao, Z. Gao, J. Jin, H. Zhou, M. Cohron, H. Zhao, H. Liu, W. Pan, Synthesis gas production with an adjustable H2/CO ratio through the coal gasification process: effects of coal ranks and methane addition, Energy & fuels 22 (3) (2008) 1720–1730.
[11] M.E. Dry, High quality diesel via the Fischer–Tropsch process – a review, J. Chem. Technol. & Biotechnol. 77 (1) (2002) 43–50.
[12] P. Jaramillo, W.M. Griffin, H.S. Matthews, Comparative Analysis of the Production Costs and Life-Cycle GHG Emissions of FT Liquid Fuels from Coal and Natural Gas, Environ. Sci. & Technol. 42 (20) (2008) 7559–7565.
[13] I. Dimitriou, P. García-Gutiérrez, R.H. Elder, R.M. Cuéllar-Franca, A. Azapagic, R. W. Allen, Carbon dioxide utilisation for production of transport fuels: process and economic analysis, Energy & Environ. Sci. 8 (6) (2015) 1775–1789.
[14] B.C.A. de Jong, K.T. Rommens, T. Rosner, P. van den Tempel, L. Rohrbach, G. L. Bezemer, H.J. Heeres, M. Saeys, C. Vogt, J. Xie, Sustainable Fuels from CO2-Rich Synthesis Gas via Fischer–Tropsch Technology, ACS Catal. 15 (12) (2025) 10946–10956.
[15] M. Ostadi, D.R. Cohn, G. Zang, L. Bromberg, Potential Expansion of Low-Carbon Liquid Fuel Production Using Hydrogen-Enhanced Biomass/Municipal Solid Waste Gasification, Sustainability 17 (13) (2025) 5718.
[16] D. Unruh, K. Pabst, G. Schaub, Fischer−Tropsch Synfuels from Biomass: Maximizing Carbon Efficiency and Hydrocarbon Yield, Energy & Fuels 24 (4) (2010) 2634–2641.
[17] Y. Gao, L. Shao, S. Yang, J. Hu, S. Zhao, J. Dang, W. Wang, X. Yan, P. Yang, Recent advances in iron-based catalysts for Fischer–Tropsch to olefins reaction, Catal. Commun. 181 (2023) 106720.
[18] A. Yahyazadeh, A.K. Dalai, W. Ma, L. Zhang, Fischer–Tropsch synthesis for light olefins from syngas: a review of catalyst development, Reactions 2 (3) (2021) 227–257.
[19] A. Karaba, J. Rozhon, J. Patera, J. Hájek, P. Zámostný, Fischer-Tropsch Wax from Renewable Resources as an Excellent Feedstock for the Steam-Cracking Process, Chem. Eng. & Technol. 44 (2) (2021) 329–338.
[20] L.P. Dancuar, J.F. Mayer, M.J. Tallman, J.J. Adams, Performance of the Sasol SPD naphtha as steam cracking feedstock, Preprints-American, Chem. Soc. Div. Pet. Chem. 48 (2003) 132–138.
[21] F. Wang, Y. Xu, J. Ren, Y. Li, Experimental investigation and modeling of steam cracking of Fischer–Tropsch naphtha for light olefins, Chem. Eng. Process. Process. Intensif. 49 (1) (2010) 51–58.
[22] P. Neuner, D. Graf, N. Netsch, M. Zeller, T.-C. Herrmann, D. Stapf, R. Rauch, Chemical Conversion of Fischer–Tropsch Waxes and Plastic Waste Pyrolysis Condensate to Lubricating Oil and Potential Steam Cracker Feedstocks, Reactions 3 (3) (2022) 352–373.
[23] K.M. Van Geem, R. Žajdlík, M.-F. Reyniers, G.B. Marin, Dimensional analysis for scaling up and down steam cracking coils, Chem. Eng. J. 134 (1) (2007) 3–10.
[24] S.P. Pyl, C.M. Schietekat, K.M. Van Geem, M.-F. Reyniers, J. Vercammen, J. Beens, G.B. Marin, Rapeseed oil methyl ester pyrolysis: On-line product analysis using comprehensive two-dimensional gas chromatography, J. Chromatogr. A 1218 (21) (2011) 3217–3223.
[25] M.R. Harper, K.M. Van Geem, S.P. Pyl, G.B. Marin, W.H. Green, Comprehensive reaction mechanism for n-butanol pyrolysis and combustion, Combust. Flame 158 (1) (2011) 16–41.
[26] M. Kusenberg, M. Roosen, A. Zayoud, M.R. Djokic, H.D. Thi, S. De Meester, K. Ragaert, U. Kresovic, K.M. Van Geem, Assessing the feasibility of chemical recycling via steam cracking of untreated plastic waste pyrolysis oils: Feedstock impurities, product yields and coke formation, Waste Manag. 141 (2022) 104–114.
[27] M. Kusenberg, A. Zayoud, M. Roosen, H.D. Thi, M.S. Abbas-Abadi, A. Eschenbacher, U. Kresovic, S. De Meester, K.M.Van Geem, A comprehensive experimental investigation of plastic waste pyrolysis oil quality and its dependence on the plastic waste composition, Fuel Process. Technol. 227 (2022) 107090.
[28] M. Kusenberg, M. Roosen, A. Doktor, L. Casado, A. Jamil Abdulrahman, B. Parvizi, A. Eschenbacher, E. Biadi, N. Laudou, D. Jänsch, S. De Meester, K.M. Van Geem, Contaminant removal from plastic waste pyrolysis oil via depth filtration and the impact on chemical recycling: A simple solution with significant impact, Chem. Eng. J. 473 (2023) 145259.
[29] Ad Klerk, Fischer–Tropsch fuels refinery design, in: Energy & Environmental Science, 4, 2011, pp. 1177–1205.
[30] T. Ishida, T. Yanagihara, X. Liu, H. Ohashi, A. Hamasaki, T. Honma, H. Oji, T. Yokoyama, M. Tokunaga, Synthesis of higher alcohols by Fischer–Tropsch synthesis over alkali metal-modified cobalt catalysts, Appl. Catal. A General. 458 (2013) 145–154.
[31] H. Du, M. Jiang, M. Zhao, X. Ma, Z. Xu, Z. Zhao, Activity and selectivity enhancement of silica supported cobalt catalyst for alcohols production from syngas via Fischer-Tropsch synthesis, Int. J. Hydrog. Energy 47 (7) (2022) 4559–4567.
[32] Y. Pei, Y. Ding, H. Zhu, H. Du, One-step production of C1–C18 alcohols via Fischer-Tropsch reaction over activated carbon-supported cobalt catalysts: Promotional effect of modification by SiO2, Chin. J. Catal. 36 (3) (2015) 355–361.
[33] Y.-P. Pei, J.-X. Liu, Y.-H. Zhao, Y.-J. Ding, T. Liu, W.-D. Dong, H.-J. Zhu, H.-Y. Su, L. Yan, J.-L. Li, W.-X. Li, High Alcohols Synthesis via Fischer–Tropsch Reaction at Cobalt Metal/Carbide Interface, ACS Catal. 5 (6) (2015) 3620–3624.
[34] A. Kharrazi, M.A. Babatabar, H. Ibrahim, A. Tavasoli, Enhancement of higher alcohols selectivity in Fischer-Tropsch synthesis using Walnut and Almond shell derived biochars as Copper/Cobalt catalyst support, J. Energy Inst. 112 (2024) 101453.
[35] T.A. Zepeda, Selectivity modulation in Fischer-Tropsch synthesis through reducibility control of cobalt-species containing HMS framework, Catal. Today 445 (2025) 115110.
[36] H.E. du Plessis, R.P. Forbes, W. Barnard, W.J. Erasmus, A. Steuwer, situ reduction study of cobalt model Fischer–Tropsch synthesis catalysts, Phys. Chem. Chem. Phys. 15 (28) (2013) 11640–11645.
[37] M.K. Gnanamani, W.D. Shafer, D.E. Sparks, B.H. Davis, Fischer–Tropsch synthesis: Effect of CO2 containing syngas over Pt promoted Co/γ-Al2O3 and K-promoted Fe catalysts, Catal. Commun. 12 (11) (2011) 936–939.
[38] Y. Yao, X. Liu, D. Hildebrandt, D. Glasser, The effect of CO2 on a cobalt-based catalyst for low temperature Fischer–Tropsch synthesis, Chem. Eng. J. 193-194 (2012) 318–327.

[39] S.-M. Kim, J.W. Bae, Y.-J. Lee, K.-W. Jun, Effect of CO2 in the feed stream on the deactivation of Co/γ-Al2O3 Fischer–Tropsch catalyst, Catal. Commun. 9 (13) (2008) 2269–2273.
[40] G. Bekmukhamedov, O. Sayidov, L. Garzón-Tovar, N. Morlanés, A. Alahmadi, R. Le Gall, J.A. Stewart, B.D. Vandegehuchte, N. Montroussier, J. Gascón, J. Ruiz-Martínez, Direct combination of RWGS and FTS for the production of fuels, Chem. Eng. J. 533 (2026) 174737.
[41] B.C.A. de Jong, K.T. Rommens, T. Rosner, P. van den Tempel, Lo Rohrbach, G. L. Bezemer, H.J. Heeres, M. Saeys, C. Vogt, J. Xie, Sustainable Fuels from CO2-Rich Synthesis Gas via Fischer–Tropsch Technology, ACS, Catalysis 15 (12) (2025) 10946–10956.
[42] P. Hirunsit, A. Senocrate, C.E. Gómez-Camacho, F. Kiefer, From CO2 to Sustainable Aviation Fuel: Navigating the Technology Landscape, ACS Sustain. Chem. & Eng. 12 (32) (2024) 12143–12160.
[43] N. Ibrić, E. Rytter, M. Hillestad, Direct conversion of CO2 and H2 to liquid fuels via Fischer–Tropsch synthesis: Novel process concept and design optimization, J. CO2 Util. 111 (2026) 103523.
[44] M. Kusenberg, G.C. Faussone, H.D. Thi, M. Roosen, M. Grilc, A. Eschenbacher, S. De Meester, K.M. Van Geem, Maximizing olefin production via steam cracking of distilled pyrolysis oils from difficult-to-recycle municipal plastic waste and marine litter, Sci. Total. Environ. (2022) 156092.
[45] S.P. Pyl, K.M. Van Geem, P. Puimège, M.K. Sabbe, M.-F. Reyniers, G.B. Marin, A comprehensive study of methyl decanoate pyrolysis, Energy 43 (1) (2012) 146–160.
[46] M. Kusenberg, A. Eschenbacher, M.R. Djokic, A. Zayoud, K. Ragaert, S. De Meester, K.M. Van Geem, Opportunities and challenges for the application of post-consumer plastic waste pyrolysis oils as steam cracker feedstocks: To decontaminate or not to decontaminate? Waste Manag. 138 (2022) 83–115.
[47] C. Delhomme-Neudecker, N. Schödel, Á. Tóta, G. Schmidt, Plastic pyrolysis oils as feedstock for steam crackers: Opportunities and challenges-Part 1, Hydrocarb. Process. (2024).
[48] N.D. Ristic, M.R. Djokic, A. Konist, K.M. Van Geem, G.B. Marin, Quantitative compositional analysis of Estonian shale oil using comprehensive two dimensional gas chromatography, Fuel Process. Technol. 167 (2017) 241–249.
[49] Y. Li, P. Watkinson, P. Herrera, F. Fahiminia, M. James, Formation of gum and deposits in an oxygenated naphtha stream, (2007).
[50] S.P. Pyl, T. Dijkmans, J.M. Antonykutty, M.-F. Reyniers, A. Harlin, K.M. Van Geem, G.B. Marin, Wood-derived olefins by steam cracking of hydrodeoxygenated tall oils, Bioresour. Technol. 126 (2012) 48–55.
[51] H. Zimmermann, R. Walzl, Ethylene, Ullmann's. Encycl. Ind. Chem. (2009).
[52] M. Kusenberg, S. De Langhe, B. Parvizi, A.J. Abdulrahman, R.J. Varghese, S. U. Aravindakshan, A. Kurkijärvi, A.M. Gandarillas, J. Jamieson, S. De Meester, Characterization and Impact of Oxygenates in Post-Consumer Plastic Waste-Derived Pyrolysis Oils on Steam Cracking Process Efficiency, J. Anal. Appl. Pyrolysis (2024) 106571.
[53] Z. Gholami, F. Gholami, Z. Tišler, M. Vakili, A review on the production of light olefins using steam cracking of hydrocarbons, Energies 14 (23) (2021) 8190.
[54] O. Herbinet, P.-M. Marquaire, F. Battin-Leclerc, R. Fournet, Thermal decomposition of n-dodecane: Experiments and kinetic modeling, J. Anal. Appl. Pyrolysis 78 (2) (2007) 419–429.
[55] K.M. Van Geem, D. Hudebine, M.F. Reyniers, F. Wahl, J.J. Verstraete, G.B. Marin, Molecular reconstruction of naphtha steam cracking feedstocks based on commercial indices, Comput. & Chem. Eng. 31 (9) (2007) 1020–1034.
[56] K.M. Van Geem, M.F. Reyniers, G.B. Marin, Challenges of modeling steam cracking of heavy feedstocks, Oil & Gas. Sci. Technol. -Rev. De. l'IFP 63 (1) (2008) 79–94.
[57] T. Dijkmans, S.P. Pyl, M.-F. Reyniers, R. Abhari, K.M. Van Geem, G.B. Marin, Production of bio-ethene and propene: alternatives for bulk chemicals and polymers, Green. Chem. 15 (11) (2013) 3064–3076.
[58] R. De Bruycker, J.M. Anthonykutty, J. Linnekoski, A. Harlin, J. Lehtonen, K.M. Van Geem, J. Räsänen, G.B. Marin, Assessing the potential of crude tall oil for the production of green-base chemicals: an experimental and kinetic modeling study, Ind. & Eng. Chem. Res. 53 (48) (2014) 18430–18442.
[59] R.De Bruycker, I. Amghizar, F.H. Vermeire, T. Nyman, M. Hakola, K.M. Van Geem, Steam cracking of bio-derived normal and branched alkanes: Influence of branching on product distribution and formation of aromatics, J. Anal. Appl. Pyrolysis 122 (2016) 468–478.
[60] N.M. Vandewiele, G.R. Magoon, K.M. Van Geem, M.-F. Reyniers, W.H. Green, G. B. Marin, Experimental and Modeling Study on the Thermal Decomposition of Jet Propellant-10, Energy & Fuels 28 (8) (2014) 4976–4985.
[61] K.M.V. Geem, I. Dhuyvetter, S. Prokopiev, M.-F. Reyniers, D. Viennet, G.B. Marin, Coke Formation in the Transfer Line Exchanger during Steam Cracking of Hydrocarbons, Ind. & Eng. Chem. Res. 48 (23) (2009) 10343–10358.
[62] L. dos S. Vargette, N.D. Ristic, M. Geerts, G.J. Heynderickx, G.B. Marin, K.M. Van Geem, Determining the fouling tendency of different feedstocks in the Fouling Assessment Setup, Heat. Mass. Transf. 60 (5) (2024) 777–784.
[63] H.M. Shirazi, L. Nelis, L. Dos Santos Vargette, G. Bellos, M. Dunkle, G. J. Heynderickx, M.-F. Reyniers, K.M. Van Geem, Unraveling the impact of temperature and feedstock composition on coke formation in steam cracking reactors, Heat. Mass. Transf. 61 (9) (2025) 80.
[64] O. Mynko, I. Amghizar, D.J. Brown, L. Chen, G.B. Marin, R.F. de Alvarenga, D. C. Uslu, J. Dewulf, K.M. Van Geem, Reducing CO2 emissions of existing ethylene plants: Evaluation of different revamp strategies to reduce global CO2 emission by 100 million tonnes, J. Clean. Prod. 362 (2022) 132127.